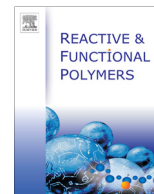




ELSEVIER

Contents lists available at ScienceDirect

Reactive & Functional Polymers

journal homepage: www.elsevier.com/locate/react

Macroporous polymers tailored as supports for large biomolecules: Ionic liquids as porogenic solvents and as surface modifiers

Diana Flor Izquierdo ^{a,1}, Malcolm Yates ^b, Pedro Lozano ^c, M. Isabel Burguete ^{a,1}, Eduardo García-Verdugo ^{a,*}, S.V. Luis ^{a,*}^a Departamento Química Inorgánica y Orgánica, Universidad Jaume I, Avda. Sos Baynat s/n, 12071 Castellón, Spain^b Departamento de Ingeniería de Procesos Catalíticos, Instituto de Catálisis-CSIC, Campus UAM-CSIC, Madrid, Spain^c Universidad de Murcia, Facultad de Química, Departamento de Bioquímica y Biología Molecular B e Inmunología, Campus de Espinardo, E-30100 Murcia, Spain

ARTICLE INFO

Article history:

Received 2 May 2014

Received in revised form 29 September 2014

Accepted 30 September 2014

Available online 8 October 2014

ABSTRACT

Highly ordered rod-like polymeric monoliths with large-pores have been successfully synthesized using ionic liquids (ILs) IL-1 (1-Butyl-3-methylimidazolium bis(trifluoromethylsulfonyl)imide [BMIM][NTf₂]) and IL-2 (1-octyl-3-methylimidazolium bis(trifluoromethylsulfonyl)imide [OMIM][NTf₂]) as alternative porogenic solvents. The presence of ILs can not only promote the formation of a highly ordered macroporous structure, control the morphology of the polymer and control the chemical composition of surfaces for monoliths prepared from DVB. In this regard, post-functionalization of the monoliths can be easily achieved using the functional monomers introduced in the polymerization process or the unreacted vinyl groups present in the polymeric matrix. This control has allowed the preparation of monolithic Supported Ionic Liquid-like Phases (m-SILLPs) with excellent morphological properties. These m-SILLPs have been studied as supports for large biomolecules. Bioadsorption studies show that the adsorbed amount of protein reaches values as high as 150–200 mg of protein per gram of support.

© 2014 Elsevier B.V. All rights reserved.

1. Introduction

Organic polymer- and silica-based monoliths have been used as good alternatives to particle-packed columns for applications ranging from highly efficient separations in capillary electrochromatography (CEC) and HPLC to preparations of supported reagents, scavengers or biocatalysts [1,2]. The small skeletons and large through-pores of the monoliths simultaneously reduce both the diffusion path length and the flow resistance, providing the advantages of low back-pressure and high mass transfer. Therefore, they are ideal materials for the development of continuous flow processes [3]. Organic polymer monoliths consisting of acrylamide-, methacrylate ester-, and styrene-based polymers have been successfully prepared [4]. However, creating a well-defined, homogeneous structure is a challenge in the preparation of monolithic materials. It is difficult to control the porous morphology of polymer monoliths prepared by traditional free radical polymerization because of the fast phase separation between the growing polymer chains and the porogenic solvents. This lack of control over the morphology of the monolith can lead to adverse effects, especially

during the flow-through processes. Thus, the outcome of the chemical processes under study can be greatly influenced by greater eddy diffusion through irregular interstitial channels, limited pore surface area and differential accessibility of the active sites [5].

Room-temperature ionic liquids (RTILs) are organic salts with melting points below 100 °C. The high modularity of RTILs allows development of an almost infinite number of compounds that are well-suited for specific applications. Recently, there have been intensive studies into the synthesis of polymeric materials in ILs as alternative solvents [6,7].

The selection of the porogenic agent is a key factor in determining the overall porosity and permeability necessary for efficient flow-through properties, which are required for continuous flow applications. The selection of the porogenic agent depends to a great extent on the intrinsic nature of the monomers. The porous structure is created by the phase separation of the rigid polymer from the porogen phase [8]. Therefore, the pore morphology obtained is a function of the solvation and composition of the monomers and porogens in the polymerization mixture. In this regard, ILs [9], including deep eutectic solvents (DESs) [10], have recently emerged as promising, single-porogenic solvents for the preparation of monolithic macroporous polymeric structures. Herein, we report on the application of neat ILs as alternative porogenic solvents to tailor the pore morphology of monoliths based

* Corresponding authors. Fax: +34 964728214.

E-mail addresses: cepeda@uji.es (E. García-Verdugo), luis@uji.es (S.V. Luis).¹ Fax: +34 964728214.

on divinylbenzene and *p*-chloromethylstyrene/divinylbenzene monomeric mixtures. These monoliths, obtained using ILs as the porogenic solvents, can be further modified by different routes to synthesize Supported Ionic Liquid-like Phases (SILLPs) [11]. This application may lead to development of materials with tunable and uniform pore systems, surfaces with tunable wet ability obtained by the functionalization with alkylimidazolium moieties, and restricted nanospaces for protein immobilization. Azoalbumin was chosen as a model of protein adsorbate to test the suitability of the macroporous material for developing advanced, supported enzymatic systems.

2. Experimental

2.1. Starting materials

Unless otherwise noted, all materials were purchased from Sigma Aldrich Chemical Company (Barcelona, Spain) and used as received. Divinylbenzene (DVB) had monomer content of 80 wt% DVB and 20 wt% ethyl-vinylbenzene (EVB). The *meta*- to *para*- isomer ratio for all monomers, including *p*-chloromethyl-vinylbenzene (purity 90%), was 70:30. The ILs used as the porogenic agents were prepared by simple ion-exchange of the commercially available chloride salts (1-Butyl-3-methylimidazolium chloride [BMIM][Cl]) or (1-octyl-3-methylimidazolium chloride [OMIM][Cl]) with LiNTf₂ [12]. *Candida antarctica* lipase type B (CALB), or Novozym 525L, was provided by Novozyme. Gases Chromatography (GC) analyses were conducted in a Varian 3900 using a CyclodexB column (length, 30 m and inner diameter, 0.25 mm).

2.2. Polymeric monolith preparation

The polymerization mixture consisted of styrene monomers (DVB or 50:50 weight mixtures of DVB and CIVB) containing different weight percentages (wt%) of the neat IL ([BMIM][NTf₂] or [OMIM][NTf₂]) used as the porogen (see Tables 1 and 2). The mass of the initiator, AIBN, was 1% of the mass of the monomers. The mixture was vortexed, sonicated and degassed until homogenous, then poured into a test tube and placed in a hot bath at 65 °C for 24 h. Next, the polymers were washed in a Soxhlet (Me-THF) to remove the unreacted starting materials and the IL.

2.3. Chemical modification of **2c** by grafting with *p*-chloromethyl-vinylbenzene

In a flask, a solution of *p*-chloromethyl-vinylbenzene (2.5283 g) in 4.0 ml of toluene and AIBN (0.0252 g, or 1% of the mass of the

monomers) were added to monolith **2c** (0.2524 g). The reaction was heated to 65 °C in a silicone bath with slow stirring for 24 h. Next, the polymers were washed with THF for 24 h in a Soxhlet to remove the unreacted starting materials. The resulting polymer was dried in a vacuum oven until the mass was constant.

2.4. Preparation of monolithic **5** and **8–11**

In a flask, the monolith to be modified (approximately 506.5 mg) and the corresponding 1-alkylimidazole (approximately 8 mL) were heated to 80 °C for 20 h. Next, the monolith was filtered and washed three times with methanol (10 mL) and dried in a vacuum oven.

2.5. Protein adsorption test for the *m*-SILLPs

The experiments measuring adsorption of azoalbumin on the macroporous polymers were conducted by mixing 2 mL of protein solution (10 mg/mL) with 10 mg of polymer. The mixture was placed in a covered vial and stirred at 25 °C. Every 30 min, a 50 µL sample was obtained for immediate analysis. The aliquots were diluted with 2 mL of water and filtered through a membrane with 0.22 µm pores. The supernatant was analyzed using UV-Vis spectroscopy to determine the protein concentration by monitoring the absorption at 385 nm. The difference in protein concentration before and after adsorption was used to estimate the amount of adsorption. The calibration curve calculated at 385 nm ($Abs = 3.51584 \times c$ (mg/mL), $R^2 = 0.99873$) was obtained using eight solutions of increasing concentrations of azoalbumin ranging from 0.05 to 0.45 mg/mL.

2.6. CALB immobilization onto SILLPs

The commercial enzyme preparation was ultrafiltered to eliminate all low-molecular-weight additives. First, 25 mL of Novozym 525L was diluted in 225 mL of water. The solution was concentrated 10-fold by ultrafiltration at 8 °C, using a Vivaflow 50 system (Sartorius) equipped with polysulphone membranes (10 kDa cut-off), resulting in a 10 mg protein/mL lipase solution. The immobilized enzyme derivatives were prepared by simple adsorption of 1 mL of an aqueous solution of CALB (10 mg/mL) onto monolith **10** (1 g). The mixture was shaken for 6 h at room temperature to adsorb the enzyme. The supernatant was recovered and the support washed with water to remove non-adsorbed enzyme. The polymer was frozen at –60 °C and lyophilized. The supernatant and washing fractions were collected and used to

Table 1
MIP analysis of the PDVB monoliths using ILs as porogen.^a

Entry	Monolith	% Weight polymerization mixture			D_{mv}^d (nm)	V_{intra}^e (cm ³ g ⁻¹)	SA ^f (m ² g ⁻¹)	P ^g (%)
		DVB	IL-1 ^b	IL-2 ^c				
1	1a	67	33	–	676	1.008	18	62
2	1b	50	50	–	643	1.013	23	65
3	1c	40	60	–	581	1.371	26	71
4	1d	33	70	–	539	2.919	36	80
5	2a	67	–	33	580	0.300	18	58
6	2b	50	–	50	694	0.576	23	66
7	2c	40	–	60	720	0.747	25	69
8	2d	33	–	70	739	0.968	30	72

Products or catalyst are marked a bold.

^a All the polymers were prepared with 1% (weight) AIBN at 65 °C during 24 h.

^b IL-1: [BMiM][NTf₂].

^c IL-2: [OMiM][NTf₂].

^d D_{mv} median pore diameter by volume.

^e V_t total intrusion volume.

^f SA: BET surface area.

^g P: porosity. % total porosity.

Table 2
BET Hg porosimetry analysis of the PCIVB-DVB monoliths using IIs as porogens.^a

Entry	Monolith	% Weight polymerization mixture			D_{mv}^d (nm)	V_T^e (cm ³ g ⁻¹)	SA ^f (m ² g ⁻¹)	P ^g (%)
		CIVB:DVB	IL-1 ^b	IL-2 ^c				
1	6a	67	33	–	844	0.882	14	49
2	6b	50	50	–	771	1.401	16	60
3	6c	40	60	–	716	1.866	17	70
4	6d	30	70	–	619	2.231	26	82
5	7a	67	–	33	873	0.877	14	38
6	7b	50	–	50	939	1.367	18	60
7	7c	40	–	60	957	1.732	16	66
8	7d	30	–	70	808	2.299	21	73

Products or catalyst are marked a bold.

^a All the polymers were prepared with a mixture 1:1 by weight of CIVB:DVB, 1% w AIBN at 65 °C during 24 h.

^b IL-1: [BMIM][NTf₂].

^c IL-2: [OMIM][NTf₂].

^d D_{mv} median pore diameter by volume.

^e V_T total intrusion volume.

^f SA: BET surface area.

^g P: porosity % total porosity.

quantify the amount of immobilized protein by Lowry's modified method (protein loading 16.5 mg per g of monolith). All the supported enzymes were stored under controlled water activity (A_w) conditions ($A_w = 0.11$) over LiCl in desiccators for 48 h at room temperature prior to use.

2.7. Batch kinetic resolution of *rac*-1-phenylethanol in hexane

Reactions were performed in 1 mL screw-capped vials with Teflon-lined septa containing 600 mL of substrate solution (450 mM *rac*-1-phenylethanol, 950 mM vinylpropionate) in dry hexanes. The reaction was started by adding the immobilized CALB (25 mg) and run with magnetic stirring at 50 °C for 8 h. At regular time intervals, 20 mL aliquots were taken and suspended in 480 mL of hexane containing 20 mM butyl butyrate (internal standard), then analyzed by GC. Profiles of (*R*)-1-phenylethylpropionate concentration with respect to time were used to quantify the reaction rates of the system. Conversion was calculated as $\%c = eeS / (eeS + eeP) \times 100$, where the subscripts S and P stand for substrate and product, respectively [13]. Enantiomeric excesses for the synthetic products were calculated as follows: $eeS = [(\%S)-12 - \%R-12] / [(\%S)-12 + \%R-12] \times 100$ $eeP = [(\%S)-14 - \%R-14] / [(\%S)-14 + \%R-14] \times 100$. One unit of synthetic activity was defined as the amount of enzyme that produces 1 mmol of (*R*)-1-phenylethylpropionate per minute. All experiments were performed in duplicate. Samples were analyzed by GC using butyl butyrate (internal standard) and the following conditions: carrier gas (He) at 107 kPa (70 mL/min total flow) and a temperature program from 60 °C till 180 °C at 10 °C /min, split ratio, 50:1; detector 300 °C.

2.8. Raman studies

Raman micro-spectroscopy was acquired using a JASCO NRS-3100 equipped with a 785 nm laser. All experiments were recorded with a resolution of 0.1 cm⁻¹. The characteristic peaks of the C=C bonds were used to determine the unreacted vinyl content of the prepared monoliths. The precision of this technique was characterized by a standard deviation ranging from 2% to 10% and an error lower than 5%. Thus, the degree of residual vinyl groups (X_C , % of double bonds) was calculated according the area (A_{rel} defined as $(A_{1630} + A_{1670-1650}) / A_{1670-1650}$). The area A_{1630} corresponds to the C=C stretching vibrations of the vinyl groups. The area $A_{1670-1650}$

corresponds to the C—C stretching vibrations of the benzene units and was used to normalize the calculation by accounting for all of the repeating units in the polymer backbone. Calibration was performed using mixtures of vinylbenzene and xylene of different compositions.

2.9. Characterization of the monoliths

The monoliths were cut into small pieces after drying under vacuum at 20 °C for 48 h. Microstructures of the dried monolith samples were observed by scanning electron microscopy (SEM) (LEO 440i, Leica-Zeiss) coupled with energy-dispersive X-ray spectroscopy (EDX) (Oxford, INCA 250). The textural characterization of the materials was conducted by the use of Mercury intrusion Porosimetry (MIP). In this technique, approximately 0.1 g of sample was placed on a sample holder and inserted in a low-pressure porosimeter (Pascal 140, Thermo Scientific). The sample was then outgassed to a vacuum of 0.1 kPa and flooded with mercury. The pressure over the mercury was then slowly increased from vacuum to 400 kPa, and the intrusion data were collected as a function of the applied pressure. Subsequently, the pressure was reduced to ambient pressure, and the sample holder was removed and weighed before being placed in the high pressure porosimeter (Pascal 240, Thermo Scientific). Next, the pressure was increased to 200 MPa while the pressure intrusion data were recorded. The high- and low-pressure data were combined and converted into cumulative pore volume versus pore diameter by use of the Washburn equation [14] with the recommended values of surface tension (484 dyne cm⁻¹) and contact angle (141°) for mercury [15]. Thus, starting under vacuum conditions and increasing the pressure to 200 MPa, the textural characteristics of the material in the pores in the range from approximately 120 μm down to 7.5 nm is determined. Analysis of the data gives rise to the cumulative pore volume, pore size distribution, bulk and skeletal densities. Assuming a cylindrical non-intersecting pore model, the intrusion data also provide an indication of the surface area of the materials by summation of the surface areas of the pore walls at each incremental pressure. With samples in the form of finely divided powders, the primary particle size distribution may also be determined by applying the Mayer Stowe theory [16] to the data obtained at the lowest pressures and widest pore diameters. In this range, the intrusion characteristics are related to the interparticulate porosity. In contrast, the characteristics of the high pressure, narrow pore diameter intrusions are related to

the intraparticulate porosity. Generally, these two ranges are easily distinguished by inflections in the cumulative intrusion curves.

3. Results and discussion

3.1. Synthesis and characterization of poly-divinylbenzene (**1** and **2**) monoliths using [BMIM][NTf₂] and [OMIM][NTf₂] as the porogenic agents

First, the synthesis of the monoliths **1a-d** and **2a-d** were assayed using two different ILs ([BMIM][NTf₂] and [OMIM][NTf₂]) as pore-forming agents. Both ILs are completely miscible with the monomer in a wide range of compositions. It was expected that the variation in the length of the cation alkyl chain may have had an effect on the architecture of the monolith. Because a single monomer was used, only the type of IL and the monomer-porogen ratio were varied. Table 1 summarizes the experimental conditions assayed for the preparation of **1a-d** and **2a-d**. The monomer-IL ratio was varied from 33 to 70% w/w.

The polymerization mixtures were poured into a mold and polymerized for 24 h at 65 °C. In all cases, the polymerization proceeded essentially quantitatively, resulting in consistent monolithic rods after the removal of the mold. The IL used as the porogen was extracted by extensive washing with Me-THF. The complete extraction of the porogen agent was monitored by Raman spectroscopy. Fig. S.I.1 depicts a representative example for **2b**. The spectrum of the monolith with the IL (bottom spectra) shows the characteristic peaks of both the polymeric backbone and [OMIM][NTf₂] that disappear after washing. For instance, peaks at 744, 1026, 1138 and 1240 cm⁻¹ corresponding to the ILs (middle spectra) are not present in the polymer after the exhaustive washing (top spectra).

To understand the relation between the synthetic conditions and the polymer morphology in terms of both pore size and pore distribution, mercury intrusion porosimetry studies were conducted for the different monoliths. The results (Fig. S.I.2 and Table 1) suggest that the pore morphology of the corresponding, cross-linked monoliths (**1a-d** and **2a-d**) can be tuned by varying the percentage and nature of the IL used as the porogenic agent. Table 1 shows that in the first series (**1a-d**), with increasing amounts of the porogen, there were increases in the intraparticulate porosity, surface area and total porosity but a decrease in the average pore width. With the second series (**2a-c**), increases in the percentage of porogen led to increases in all of the other parameters, including average pore diameter, intraparticulate pore volume, surface area and porosity. Both series of polymers, synthesized using either [BMIM][NTf₂] or [OMIM][NTf₂], have larger mean pore size and narrower size distribution than the ones reported for the polymerization of DVB using toluene as the porogen (56 nm of median pore diameter by volume, BET surface area 321 m² g⁻¹) [17].

The total porosity of these monoliths varies from 60% to 80% when the amount of [BMIM][NTf₂] used is increased from 30% to 70% (Table 1, entries 1–4), while the use of [OMIM][NTf₂] only leads to a variation from 60% to 70% (Table 1, entries 5–8). The surface area of the monoliths only reaches modest values of 18–38 m² g⁻¹ in good agreement with the fact that these monoliths are highly macroporous materials.

The microstructures of the dried monolith samples observed by SEM (Fig. S.I.3) confirmed the distributions obtained by MIP, where the interparticulate porosity was due to filling between the spherical globules, and the intraparticulate porosity was due to the pore structure within these particles. The SEM images showed that the skeletons of the monoliths were formed by connected globular particles forming regular conglomerates. Thus, the main

pore component (500–700 nm) is formed by the void volume among the connected globular particles. Furthermore, the micrometer-sized pores, which facilitate low-resistance flow through the three-dimensional network, are the result of the packing of the conglomerates formed by cross-linked polymer globular particles. It is noteworthy that the main pore component within the nanometer-size was proportional to the amount of IL used.

3.2. Synthesis and characterization of Poly(*p*-chlorovinylbenzene-co-divinylbenzene) (**6** and **7**) monoliths using [BMIM][NTf₂] or [OMIM][NTf₂] as the porogenic agent

Using methods similar to those described in the previous section, different functionalized polymers bearing chloromethyl groups were prepared using a 1:1 mixture (by weight) of the monomers *p*-chloromethylstyrene and divinylbenzene with different percentages of the corresponding ILs ([BMIM][NTf₂] or [OMIM][NTf₂]) as the porogen. Table 2 summarizes the experimental conditions, composition and results obtained through analysis of these materials by mercury porosimetry.

Once again, highly porous polymers were obtained, showing the same porosity range found for the monoliths prepared with only DVB. Again, the mean pore diameter was related to the amount of IL used. However in this case, an increase in the percentage of IL (from 30% to 70%) resulted in a decrease in the mean pore diameter by volume from 844 nm to 619 nm. Nevertheless, there were increases in the intraparticulate porosity, surface area and porosity. These results were similar to those obtained in the first series with this porogen. (Table 1, entries 1–4).

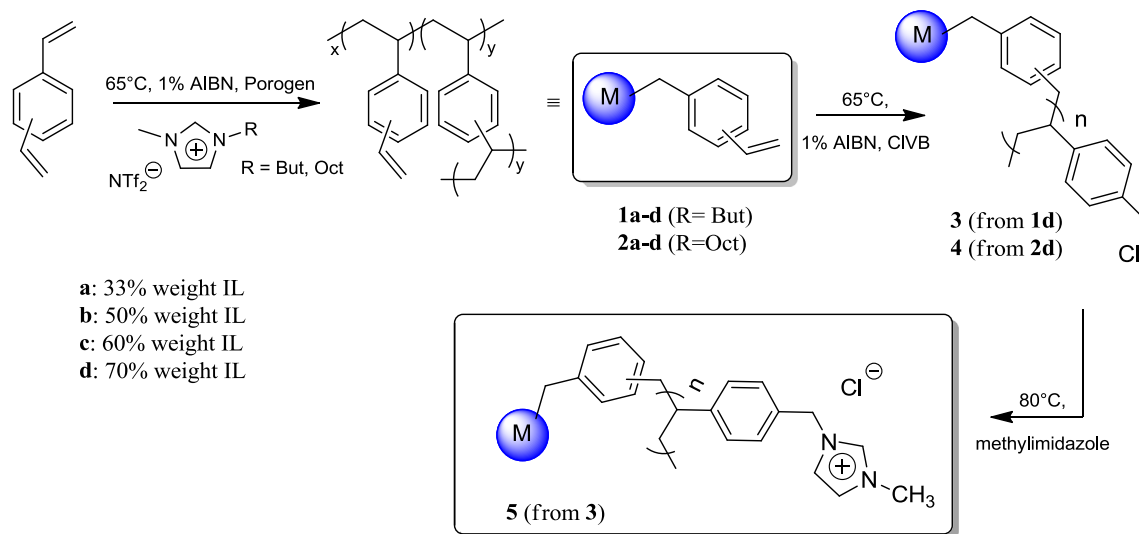
Finally, when [OMIM][NTf₂] was used as the porogen, a linear relationship between the mean pore diameter by volume and the amount of IL used was observed for the monolith. The monoliths (**6a-b**) presented a monomodal pore size distribution from 30% to 60% of IL). Thus, larger mean pore diameters were observed when higher percentages of IL were used in the mixture. This trend was broken for the polymer prepared using 70% IL (**6c**), which presented a bimodal pore size distribution (Fig. S.I.4).

It seems clear that the morphology of the monoliths prepared by the polymerization of DVB or CIVB:DVB is quite sensitive to small changes in the amount and nature of the ILs used as porogens. Thus, the use of ILs as porogens provides a simple and exciting approach to tuning the structural characteristics of macroporous polymer monoliths. The advantage of this methodology is that a small change in the IL, in this case having either butyl or octyl side chains, leads to significant variation in the final morphology, providing multiple opportunities for the fine-tuning of the polymeric morphology. Indeed, the variation in the nature of the ILs, similar to the already-reported effects for conventional organic solvent porogens, can significantly impact the mechanism of phase separation, nucleation and aggregation processes that influence pore formation [18].

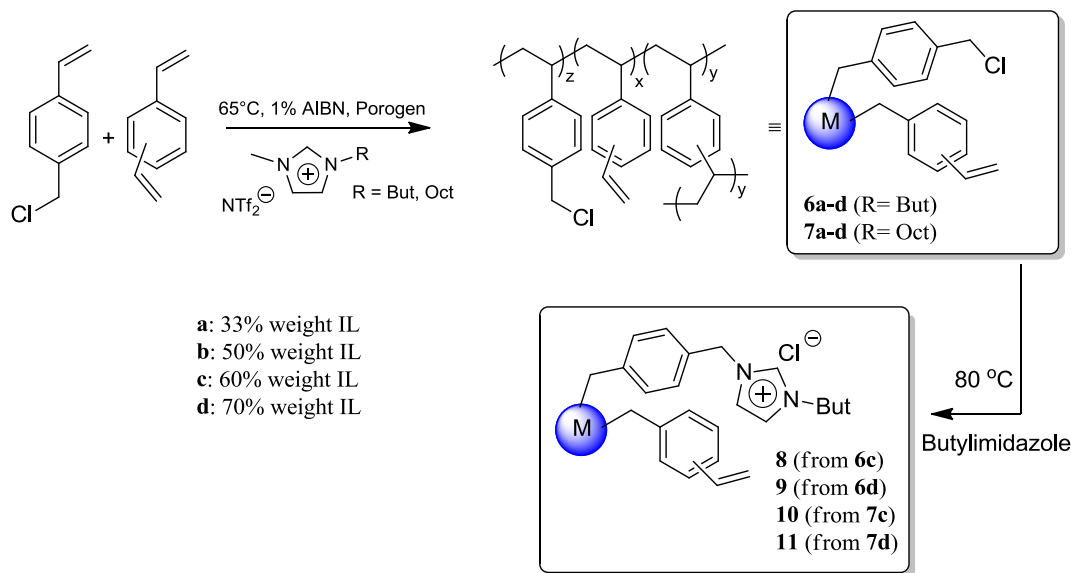
To evaluate the impact of the ILs as porogens on the properties of these polymers as potential materials for various applications, we have further studied these monoliths for the preparation and use of the so called Supported Ionic Liquid-Like Phases (SILLPs) using several approaches.

3.3. Chemical surface modification of Poly(divinylbenzene) monoliths (PDVB) for the synthesis of SILLPs

Polymers prepared by conventional polymerization of DVB (for instance, XAD-4) contain a significant amount of residual vinyl content, ranging from 29–40% [19]. These reactive sites can be used to attach either functional groups or new polymer chains to the surface of the resin (Scheme 2) [20]. Modification of the resins by grafting reactive polymers inside the pores of macroporous



Scheme 1. Synthesis of PDVB monoliths by bulk polymerization of DVD (80% grade) using ILs as porogenic solvents and further chemical modification to prepare the related *m*-SILLP.



Scheme 2. Synthesis of PCIVB-DVB monoliths by polymerization of a mixture CIVB: DVD (1:1) using ILs as porogenic solvents and their further modification to synthesize *m*-SILLPs 8–11.

supports is highly interesting [21] because the residual vinyl groups of the monoliths can be used to introduce new *poly* (*p*-chloromethylstyrene) chains. Further modification of these chains with alkyl imidazole will produce SILLPs (Scheme 1).

Raman micro-spectroscopy was used to identify the degree of residual vinyl content of the monoliths prepared with ILs as porogens. Raman micro-spectroscopy is a powerful tool for providing both qualitative and quantitative data. In all cases, the Raman spectra of the different PDVB monoliths revealed the presence of these reactive sites. The presence of vinyl groups presence can be easily monitored through the analysis of the characteristic peak at 1631 cm^{-1} , assignable to the C=C stretching vibrations of the remaining vinyl groups [22]. A calibration was performed to quantitatively determine the presence of this group. Different mixtures of vinylbenzene were used as equivalents of the unreacted olefin and xylene was used as an analog of the polymeric backbone. The representation of the normalized area of the peak at

1630 cm^{-1} was compared with the composition of the calibration sample, and good quantitative correlation was observed. This correlation allowed the residual vinyl content to be determined in the different monoliths prepared (Table 3). The monoliths prepared using [BMIM][NTf₂] did not show any significant change in the loading of the vinyl groups (ca. 20%) or, therefore, in the degree of crosslinking with the increase in the amount of the IL used (Table 3, entries 1–4). Thus, within the error of the determination, the degree of remaining vinyl groups on the surface of these monoliths is almost constant. In contrast, for the monoliths prepared using different contents of [OMIM][NTf₂], a significant variation in the vinyl content (from ca. 10% to ca. 20%) was observed. Thus, ILs can be used not only to tune the morphology of the polymer but also the chemical composition on the monolithic surface.

Once the presence and amount of vinyl groups on the surface of the monoliths was determined, the possible modification of the groups was also evaluated. The modification was performed by

Table 3
Vinyl content of PDVB monoliths using ILs as porogens.^a

Entry	Monolith	% Weight pol. mixture			Degree of functionalization	Degree of crosslinking	Vinyl content (mmol g ⁻¹) ^c
		DVB	IL-1 ^b	IL-2 ^c	X _{VB} (%) ^a	X _{Cl} (%) ^b	
1	1a	67	33	–	21	59	1.59
2	1b	50	50	–	19	61	1.50
3	1c	40	60	–	18	62	1.35
4	1d	33	70	–	20	60	1.52
5	2a	67	–	33	19	61	1.42
6	2b	50	–	50	14	66	1.07
7	2c	40	–	60	12	68	0.91
8	2d	33	–	70	11	69	0.86

Products or catalyst are marked a bold.

^a Calculated by FT-Raman.

^b X_{Cl} = (%) DVB – X_{VB}.

^c Vinyl content (mmol/g) = (X_{VB}/avg. MW) × 10. The molecular weights of the monomers are 130.2 g/mol for DVB, and 132.2 g/mol for ethylvinylbenzene, thus for DVB 80% grade the avg. MW per repeat unit = g/mol (0.8 × 130.2 + 0.2 × 132.2) = 130.6 g/mol.

suspending monolith **1d** in a mixture of 10% (by weight) *p*-chloromethylstyrene in DMF at 65 °C for 24 h [23]. Next, the polymer was thoroughly washed to remove all possible soluble polymers and oligomers or unreacted monomers not grafted to the monolith surface. The Raman spectra of the modified monoliths showed the presence of the characteristic peaks for the chloromethyl groups at 1261 and 682 cm⁻¹ and a reduction in the intensity of the peak at 1630 cm⁻¹, characteristic of the C=C bond. The decrease in the 1630 cm⁻¹ band indicates a decrease in the vinyl groups from 19% to 14%. The spectra also showed an increase in the intensity of the peaks characteristic of the *para*-aromatic rings di-substitution at 1209 and 1181 cm⁻¹.

These results suggest that the unreacted C=C bonds on the surface of the polymer are sufficiently reactive to perform a chemical modification by grafting polymerization. Although the degree of the substitution is not high, the fact that these groups are present in the most accessible regions of the monoliths is crucial for developing further applications. Indeed, these functional groups are accessible enough to react quantitatively by a methodology previously reported by us, which involves the reaction of methylimidazole with the -CH₂-Cl groups of the polymer to yield the corresponding polymeric ionic liquid-like fragments on the surface of polymer **5** (Scheme 1). Elemental analyses confirmed the total functionalization of the monolith, affording polymers with approximately 0.4 mmol of IL-like units per gram of monolith. This loading is in the range of those previous reported for similar modification process of the monoliths that were prepared using conventional porogenic mixtures of toluene and dodecanol [23]. Thus, the accessibility of the unreacted vinyl groups obtained using a single IL as the porogenic agent is similar to those achieved for monoliths obtained using conventional systems, which usually require at least a mixture of two components as the porogenic agent.

3.4. Chemical modification of poly(chloromethyl-co-divinylbenzene) monoliths PCIVB-DBV (6 and 7) for the synthesis of SILLPs

Some of the PCIVB-DBV monoliths were reacted with butylimidazole to evaluate the suitability of these materials, which were prepared with ILs as porogens, for the preparation of SILLPs according to Scheme 2. The modification of the polymers can be quantitatively monitored by taking resin samples at different time intervals and analyzing them by means of Raman micro-spectroscopy. A monolith prepared using a conventional toluene and dodecanol mixture as the porogen was also used as a control experiment (**12**). Fig. S.I.7 depicts the functionalization process of the monoliths **6c** and **12** with butylimidazole at 80 °C. The variation of the peak at 1265 cm⁻¹ (corresponding to the wagging bands

of CH₂-Cl) with the reaction time provides information on the substitution of these groups with the IL-like moieties (kinetics profiles). However, no important differences were observed between the kinetic profiles of monoliths **6c** and **12**. This result suggests that both methods for monolith preparation, using conventional solvents and ILs as porogens, lead to functional sites with similar accessibility for substitution. In general, for the synthesis of the different SILLPs, good yields could be achieved for all the considered transformations. This is clearly illustrated by the data shown in Table 4, which shows the values obtained for conversion and loading for the final SILLPs from the corresponding elemental analysis data. Yields were determined by comparing the actual nitrogen content of the polymers to that expected for a 100% conversion. The substitution does not reach 100% because some functional groups are located in the highly cross-linked region, where they are less accessible. The results once again highlighted that the properties of the monoliths obtained using ILs as the porogen are comparable to the monoliths obtained with more complex conventional systems.

3.5. Evaluation of the monolithic SILLPs as protein supports

The different monolithic SILLPs prepared were tested as supports to adsorb biomolecules, particularly azoalbumin. PS-DVB macroporous monoliths are suitable carriers for enzymes due to their hydrophobic nature, which facilitates interfacial activation of the enzyme to the hydrophobic surface of the support [24]. However, the low wettability of these materials may hinder the adsorption of enzymes in aqueous solution. The modification of the monoliths with IL-like moieties enables tuning of the surface wettability and their compatibility with water. These modifications facilitate the adsorption and transfer of bulky enzymes onto the surface of monolithic SILLPs. Indeed, unmodified monoliths show very poor wettability (Fig. 1b). The hydrophobicity of these materials does not allow water to diffuse through their

Table 4
Loading of the IL-like moieties obtained for the *m*-SILLPs.^a

Entry	From	<i>m</i> -SILLP	Loading exp. ^b (mmol LI/g)	Loading theo. ^c (mmol LI/g)	Yield (%)
1	6c	8	2.36	2.57	92
2	6d	9	2.26	2.57	88
3	7c	10	2.31	2.57	90
4	7d	11	2.35	2.57	91

Products or catalyst are marked a bold.

^a Values obtained after 24 h of reaction time.

^b Calculated by elemental analysis.

^c Theoretical values based on the monomeric composition.

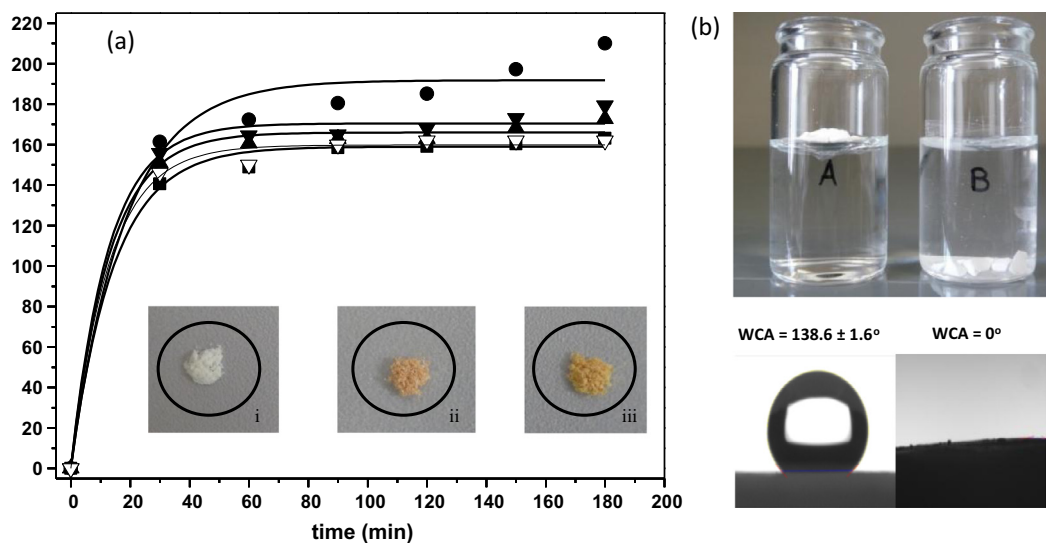


Fig. 1. (a) Adsorption capacity at pH 7.0 azoalbumin on **5** and **8–11**. (∇) **5**; (\blacksquare) **8**; (\blacktriangledown) **9**; (\bullet) **10**; (\blacktriangle) **11**. Insets: difference on the coloration of monoliths exposed to the azoalbumin for 3 h. (i) **6c**, (ii) **5** and (iii) **8**. bSt Comparison of the wettability in water and contact angle of (A) **6c** and (B) **8**.

macroporous structure. Therefore, when the monolith is immersed in water, the polymer floats to minimize the contact with the aqueous phase because of the high surface tension between the polymer and the water (Fig. 1b). After the modification of the monolith with N-alkylimidazole, the surface of the polymer was covered with ionic, liquid-like units with chloride as the anion. Because this is a much more compatible functionality for water, the water diffused through the pores, and the filled monolith was drawn by gravity to the bottom of the vial. Indeed, the evaluation of the wetting behavior by the water contact angle (WCA) on the surface of the monolithic materials confirmed the change in polarity of the polymers. As shown in Fig. 1b, the unmodified polymer (**6c**) displayed a WCA of $138.6 \pm 1.6^\circ$, indicating its ultrahigh hydrophobic character. This result is expected because the polystyrene backbone of the polymer is intrinsically hydrophobic. However, after modification of the monolith with butylimidazole (**8**), it was observed that the water droplet was rapidly absorbed on the polymer surface within several seconds ($\text{WCA} = 0^\circ$). This change in the compatibility with water is reflected in the capacity of these porous materials to adsorb azoalbumin. Indeed, the unmodified monoliths were not able to adsorb any protein, even after extensive contact time. This property is reflected in the fact that the materials did not show any coloration (Fig. 1a, i). In contrast, all the monoliths modified with ionic liquid-like units efficiently adsorbed azoalbumin, displaying the characteristic coloration (Fig. 1a, ii and iii). Fig. 1a depicts the adsorption profile obtained for the different SILLPs assayed. The monoliths did not show significant differences in the adsorption capacity reaching

values of approximately 150–200 mg of protein per gram of support. The equilibrium was achieved after one hour, and the only material showing a slightly different profile was monolith **10**, which required a longer adsorption time to reach equilibrium. However, monolith **10** was also able to adsorb a larger amount of protein (212 mg of protein per gram of polymer). The relatively large amount of protein immobilized onto the SILLPs can be attributed to their large pore sizes, which allow excellent diffusion from the solution to the pores. Weak interactions such as hydrogen bonding, hydrophobic and van der Waals attractions, and ionic interactions, which all contribute to the immobilization of large proteins, would favorably converge using this approach. These types of interactions are usually too weak to prevent enzyme molecules from leaching into the reaction media, but the multiple, additive and multidimensional interactions at work in the case of SILLPs are clearly effective for this purpose (see Table 5).

3.6. Stability of the absorbed proteins onto the monolithic SILLPs as protein support

To evaluate the stability of the protein adsorbed onto the SILLPs, the immobilization of the lipase B from *C. Antarctica* (CALB) was assayed. Monolith **10**, which showed the largest protein adsorption capacity, was selected for this purpose. It is well known that changes in the 3D-structure of CALB can lead to its inactivation as a biocatalyst. Thus, protein structural changes that occur during adsorption of the enzyme can be easily followed by assaying the catalytic activity of a given model reaction (e.g., kinetic resolution of *rac*-1-phenyl-ethanol). By placing a solution of CALB in water in contact with monolith **10**, CALB was adsorbed onto the monolith. The activity of the immobilized protein on monolith **10** (loading 16.5 mg/g) was tested in the resolution of *rac*-1-phenyl-ethanol. The system showed excellent activity, leading to 49% conversion of **12**. The system also showed excellent enantioselectivity corresponding to an acylated product (**13** > 99% *e.e.*) and an activity of 195 U/g support ($U = (\mu\text{mol}/\text{mL}) \times \text{min}^{-1}$). This result is comparable to those found with analogous systems and for commercial biocatalysts [25]. This result confirmed that non-deactivation happens under protein immobilization. Regarding the long-term stability of the immobilized protein, it should be noted that both the activity and the enantioselectivity of this supported biocatalyst remain

Table 5
Azoalbumin loading for the different *m*-SILLPs.

Entry	Support	D_{mv}^a (nm)	SA^b ($\text{m}^2 \text{g}^{-1}$)	Immobilized. protein (%) ^c	mg protein/g support
1	5	677	38	41	162
2	8	716	17	42	163
2	9	619	26	45	179
3	10	957	16	54	212
4	11	808	21	41	173

^a D_{mv} median pore diameter by volume.

^b SA: BET surface area.

^c Protein adsorbed after 3 h.

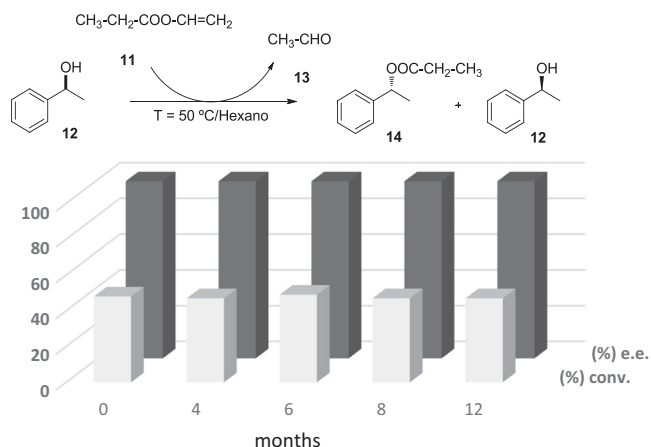


Fig. 2. Stability profile vs. time for catalytic performance of the CALB supported on monolith 10.

unchanged for a period of at least one year (see Fig. 2). No special care is needed to maintain the activity except to store it under controlled water activity (A_w) conditions ($A_w = 0.11$) over LiCl in a desiccator. This behavior is indicative of extraordinarily long-term stability of the immobilized protein in the monolithic materials. This behavior is in good agreement with the previous results for this type of material observed even when more air-sensitive organometallic catalysts are immobilized onto monoliths [26–28].

4. Conclusions

The use of ILs as porogenic agents for the preparation of macroporous monolithic polymers presents some distinct advantages. First of all, the morphology and porous structure of the resulting monoliths can be easily tailored through a proper selection of the structural features of the IL. The resulting monoliths have been shown to present narrower pore distributions in the region of interest for the development of continuous-flow applications. The mean pore diameter can be selected by modifying the amount of IL used. Furthermore, the use of ILs as porogenic agents can favor the location of the reactive groups of the polymer at the most accessible sites on the polymeric surfaces, facilitating its further modification. Our results show how functional polymers containing chloromethyl groups and having the desired morphological properties can be easily obtained through the copolymerization of DVB with CIVB or by grafting of CIVB onto the surface of PDVB monoliths. These methods take advantage of the reactivity and accessibility of the unreacted vinyl groups present in PDVB. Further reaction of the resulting chloromethyl functionalities with an alkyl imidazole produces macroporous polymers with surfaces modified with IL-like fragments (imidazolium subunits) that can be used to greatly modify the properties of the resulting polymers. The important potential applications of the resulting materials have been exemplified by their use as supports for large biomolecules such as azoalbumin, which can be adsorbed very efficiently on these monoliths. It must be noted that the amount of protein that can be immobilized in a simple way on the present materials (SILLPs)

is much larger than that usually found for other standard supports for biomolecules. These types of supports are considered interesting applications for the immobilization of enzymes. Hence, the SILLPs prepared by the methodology reported here are excellent supports for lipase (CALB), showing good biocatalytic activity. Furthermore, the monolithic SILLPs provide an excellent long-term stability to the support system. This work clears the way for developing new applications based in the support of large biomolecules and, in particular, those involving continuous flow processes.

Appendix A. Supplementary data

Supplementary data associated with this article can be found, in the online version, at <http://dx.doi.org/10.1016/j.reactfunctpolym.2014.09.026>.

References

- [1] R.Y. Zhang, L. Qi, P.R. Xin, G.L. Yang, Y. Chen, *Polymer* 51 (2010) 1703–1708.
- [2] F. Svec, T.B. Tennikova, Z. Deyl, *Monolithic materials: preparation, properties and application*, J. Chromatogr. Libr., vol. 67, Elsevier, Amsterdam, 2003.
- [3] S.V. Luis, E. Garcia-Verdugo, *Chemical Reactions and Processes under Flow Conditions*, Royal Society of Chemistry, Cambridge, 2009.
- [4] J. Sproß, A. Sinz, *J. Sep. Sci.* 34 (2011) 1958–1973.
- [5] V. Sans, N. Karbass, M.I. Burguete, E. Garcia-Verdugo, S.V. Luis, *RSC Adv.* 2 (2012) 8721–8728.
- [6] (a) P. Kubisa, *Prog. Polym. Sci.* 34 (2009) 1333–1347; (b) P. Kubisa, *J. Polym. Sci. A* 43 (2005) 4675–4683.
- [7] T. Erdmenger, C. Guerrero-Sanchez, J. Vitz, R. Hoogenboom, U.S. Schubert, *Chem. Soc. Rev.* 39 (2010) 3317–3333.
- [8] (a) F. Svec, J.M.J. Fréchet, *Chem. Mater.* 7 (1995) 707–715; (b) C. Viklund, F. Svec, J.M.J. Fréchet, K. Irgum, *Chem. Mater.* 8 (1996) 744–750.
- [9] a) Y.-H. Shih, B. Singco, W.-L. Liu, C.-H. Hsu, H.-Y. Huang, *Green Chem.* 13 (2011) 296–299; b) B. Singco, C.-L. Lin, Y.-J. Cheng, Y.-H. Shih, H.-Y. Huang, *Anal. Chim. Acta* 746 (2012) 123–130.
- [10] D. Carriazo, M.C. Serrano, M.C. Gutiérrez, M.L. Ferrer, F. Del Monte, *Chem. Soc. Rev.* 41 (2012) 4996–5014.
- [11] V. Sans, N. Karbass, M.I. Burguete, V. Compañ, E. García-Verdugo, S.V. Luis, M. Pawlak, *Chem. Eur. J.* 17 (2011) 1894–1906.
- [12] P. Nockemann, K. Binnemans, *Chem. Phys. Lett.* 415 (2005) 131–136.
- [13] C.S. Chen, Y. Fujimoto, G. Girdaukas, C.J. Sih, *J. Am. Chem. Soc.* 104 (1982) 17294.
- [14] E.W. Wasburn, *Phys. Rev.* 17 (1921) 273.
- [15] K.S.W. Sing, D.H. Everett, R.A.W. Haul, L. Moscou, R.A. Pierotti, J. Rouquerol, T. Siemieniowska, *Pure Appl. Chem.* 57 (1985) 603.
- [16] R.P. Mayer, R.A. Stowe, *J. Colloid Interface Sci.* 20 (1965) 893.
- [17] P. Snedden, A.I. Cooper, K. Scott, N. Winterton, *Macromolecules* 36 (2003) 4549–4556.
- [18] D.C. Sherrington, *Chem. Commun.* (1998) 2275–2286.
- [19] K.L. Hubbard, J.A. Finch, *React. Funct. Polym.* 36 (1998) 17.
- [20] K.L. Hubbard, J.A. Finch, G.D. Darling, *React. Funct. Polym.* 36 (1998) 1.
- [21] (a) E.C. Peters, F. Svec, J.M.J. Fréchet, *Talanta* 79 (2009) 739; (b) J.A. Tripp, F. Svec, J.M.J. Fréchet, *J. Comb. Chem.* 3 (2001) 216; (c) C. Viklund, F. Svec, J.M.J. Fréchet, K. Irgum, *Biotechnol. Progr.* 13 (1997) 597; (d) X.Y. Wei, L. Qi, G.L. Yang, F.Y. Wang, *Talanta* 79 (2009) 739.
- [22] B. Altava, M.I. Burguete, E. Garcia-Verdugo, S.V. Luis, M.J. Vicent, *Tetrahedron* 57 (2001) 8675–8683.
- [23] J.A. Tripp, T.P. Needham, E.M. Ripp, B.G. Konzman, P.J. Homnick, *React. Funct. Polym.* 70 (2010) 414–418.
- [24] R.A. Sheldon, *Adv. Synth. Catal.* 349 (2007) 1289–1307.
- [25] P. Lozano, E. Garcia-Verdugo, N. Karbass, K. Montague, T. De Diego, M.I. Burguete, S.V. Luis, *Green Chem.* 12 (2010) 1803–1810.
- [26] B. Altava, M.I. Burguete, E. Garcia-Verdugo, S.V. Luis, M.J. Vicent, *Green Chem.* 8 (2006) 717–726.
- [27] B. Altava, M.I. Burguete, E. Garcia-Verdugo, S.V. Luis, M.J. Vicent, J.A. Mayoral, *React. Funct. Polym.* 48 (2001) 25–35.
- [28] D. Kundu, A.K. Patra, J. Sakamoto, H. Uyama, *React. Funct. Polym.* 79 (2014) 8–13.